Evaluation of the power of Dark Photon searches at the ILC

Author
Josh GREAVES

Supervisors
Jenny LIST
Mikael BERGGREN

Conducted
Summer 2021

ABSTRACT

It is evident from cosmological observations such as the Cosmic Microwave Background, and the motion of galaxies, that the universe consists of approximately 5 times more mass than visible matter can account for. FIPS (Feebly Interacting ParticleS) are candidates for this dark matter, and could explain their lack of detection at current accelerators. Cosmological constraints based on the abundance indicate that dark matter particles could be too weakly interacting to have been observed at LHC or LEP but, with up to 1000 times greater luminosity, future e+e- machines such as the International Linear Collider (ILC) open up new ways to search.

This project will study the scenario where the dark matter model in question contains a dark photon, which decays into SM particles; more specifically to muon pairs. The signal to search for is a very small and narrow peak in the the di-muon spectrum, though it is not known exactly where. The limits on the detection of such a peak, at the ILC, are to be explored.

In conjunction with another student who will be generating the signal, and conducting the fast detector simulation of it, this project will estimate the background rates using full detector simulation, with the aim of deriving the discovery and exclusion potential of the ILC in this scenario.

LUND UNIVERSITY

Contents

1 Introduction and Motivation

Of the unanswered questions facing us in elementary particle physics, the question of *dark matter* is high on the list. Cosmological observations have confirmed its existence as a gravitationally interacting material, but the question of where dark matter came from, and its specific nature, still requires an answer. Could dark matter interact with normal matter? Were they coupled somehow at some point in universal history?

One long standing candidate for dark matter beyond the Standard Model is the *WIMP - Weakly Interacting Massive Particle*. WIMPs are anything above a few GeV in mass to TeV mass scales with a coupling similar to that of the weak interaction. FIPs theoretically couple more strongly than WIMPs, which according to the current relic abundance, requires them to have a lower mass; something in the sub GeV range. This puts their associated gauge bosons, the dark photons, in the range of intensity frontier facilities like the ILC.

Detection of dark matter has been unsuccessful so far through direct and indirect detection; detecting the recoil of Standard Model particles through interactions with dark matter, and the search for decay products such as gamma rays. That leaves indirect methods such as at the ILC, in which dark matter could be produced in collisions of Standard Model leptons.

The apparent abundance of dark matter is linked to its behaviour in the early universe, particularly its interaction with standard matter. In fact, the rate of interaction between standard and dark matter could have gone to zero, and the amount of dark matter could have been *frozen out* at some point, meaning that due to the increasing Hubble expansion rate since the big bang, a point was reached where dark and standard matter became decoupled, leading to a constant relic abundance of dark matter in the universe from that point, which we see today. This non gravitational dark matter interaction scenario is well motivated and compelling because of its simplicity. Using the current abundance of dark matter, one can work backwards and discover a constrained mass range for possible dark matter particles.

To investigate potential non gravitational interactions requires exploration of specific energy ranges. The ILC will initially have a maximum centre of mass energy of 500GeV, with a potential capacity in the future to upgrade to 1000GeV[1] by 'simply' building onto the existing tunnel, and adding more RF cavities to further accelerate the electrons and positrons.

In comparison with the circular Large Hadron Collider(LHC), the attainable centre of mass energies at ILC are limited by the length of these RF cavities, as opposed to the energy at the LHC being limited by the power of the bending magnets around the ring. This begins to highlight the complementarity between the two accelerators and their configurations. The centre of mass energies at the LHC can reach 13TeV[2], approximately 26 times that of the ILC initially at 500GeV. Even though the tunnel length of the ILC, at 31km[1], is comparable to the LHC circumference of 27km, these attainable energies are so different because of the principle of conservation of momentum for an accelerated charged particle. Since a charged particle undergoes constant acceleration when moving in circular motion, for example around the LHC ring, it will experience an acceleration and a momentum change. An emitted photon is therefore required to compensate for this, and so we have the principle that an accelerating charged particle will emit radiation, known as *Synchrotron radiation*. These radiated photons reduce the kinetic energy of the particles as they traverse the ring. For hadrons, such as protons, which are almost 2000 times heavier than electrons, this kinetic energy loss is nowhere near as substantial and can be accounted for by the RF cavities. For an electron, this would not be possible and would require far too much energy. So, hadrons can be accelerated around the LHC to high energies, and collided together, whereas lighter leptons require linear acceleration to reach high collision energies.

Since protons are composite particles containing many different partons, such as strongly interacting quarks with an associated parton distribution function, the initial states are not well known. This leads to far more complicated final states, albeit at higher energies. For this reason, the LHC is more of a *discovery* machine. At the ILC, the electrons and positrons only interact electromagnetically, and since they are point particles, they have well defined initial states and lead to much more precise final states and analysis. Therefore, the ILC is a *precision* machine, and thereby complements the LHC in fundamental physics measurements.

In the scenario relevent to this project, the dark photon decays into SM particles (Figure 1), specifically to muon pairs. The electron positron pair system may be reduced in energy by the emission of an Initial State Radiation (ISR) photon, meaning the signature would be one photon and two leptons. The signal is then expected to be a very narrow peak in the the di-muon spectrum, the question is, where?

Muons are the best particles to seek in this case because, while the decay products could indeed be hadronic in nature, these could be neutral, meaning they are not measurable. Muon detection resolution is also much higher in comparison to calorimeter resolution, and we will want to use as narrow a window as possible to reduce the amount of background that will be captured. Furthermore, muon pairs are additionally preferable to electron pairs due to the aforementioned bremsstrahlung of electrons. This radiation by electrons will cause their peak to be wider in the calorimeter, meaning we would require a wider window than for muon pairs. We could theoretically obtain double the statistics by considering electron pairs, at the expense of having this wider peak.

For the backgrounds to this process, we have a database of output data from full detector simulation in the form of DST files; this is a standard format used by linear collider event data models. In this case, we are using ILCsoft and Linear Collider I/O (LCIO)[3]. The principle aim was to create code that would plot the backgrounds of the muon mass spectrum from this data for relevant processes, before combining this analysis with a dark photon signal generated by the Whizard[4] Monte Carlo event generator. This enables the derivation by statistical analysis of the discovery and exclusion potential for the ILC in this scenario. The dominant background is the 2-fermion leptonic decay of the Z resonance, shown in Figure 2.

2 Simulation

2.1 Backgrounds and cuts

Using the full Monte Carlo (MC) simulation of detector systems in the LCIO framework [3], the output files are in the DST format. DST files contain collections of reconstructed data separated into events. The primary DST files are compared below in Table 1 with a processed version known as miniDST. This contains extra collections which are useful for analysis, especially in making cuts to remove backgrounds. The Particle Flow Objects (PFOs) contain all reconstructions. The isolated leptons are subsets of this PFO collection.

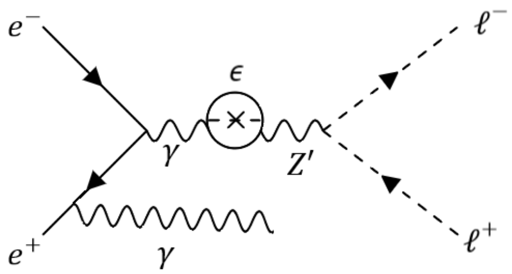

Figure 1: Feynman diagram signal - production of Z', including ISR photon, and following decay to lepton pair.

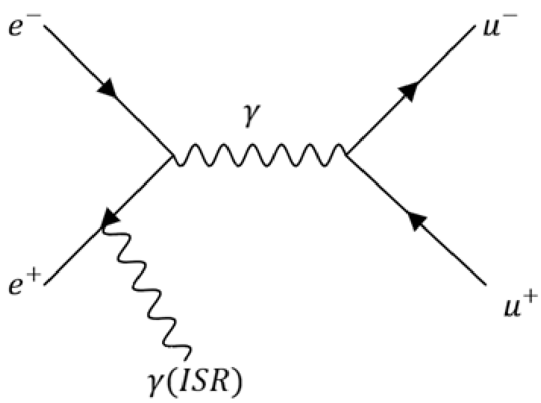

Figure 2: Feynman diagram - Muon pair production an ISR photon

The Jet collections are the PFO set minus the isolated leptons, and then forced into 2,3,4,5 or more jets.

Table 1 Comparison between data collections in DST and miniDST files

DST	**miniDST**
Pandora PFOs	Pandora PFOs
MC Particles	MC Particles
Vertex data	Vertex data
-	Isolated reconstructed leptons/photons
-	Refined Jet collections

My starting point was to plot the dimuon mass spectrum for the isolated muon collection, considering only pairs of oppositely charged muons, in a set of 2-fermion leptonic miniDST files. This again corresponds to the diagram shown in Figure 2, and the plot is shown in Figure 3.

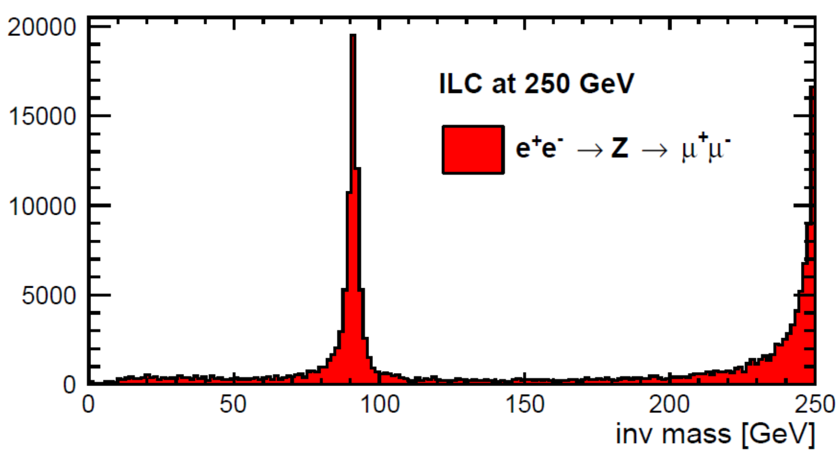

Figure 3: Z resonance producing Dimuons (isolated muon collection only), showing Z mass peak at ≈ 91GeV, and muon pair with shared CoM energy 250GeV. Boosted muons at ≈ 10GeV are cut at generator level.(Average of 14 PFOs per event)

I next explored some ways to potentially cut out other backgrounds. For example, Figure 5 shows the previous plot with 4-fermion semileptonic data stacked on top of it. One can observe that there are no muon pairs ramping up toward sharing the centre of mass energy in this case, since the quarks will have removed some of the energy, making this impossible. The muons which do share the centre of mass energy in the 2-fermion example correspond to cases where an ISR photon was not released. The corresponding Feynman diagram for this is shown in Figure 4.

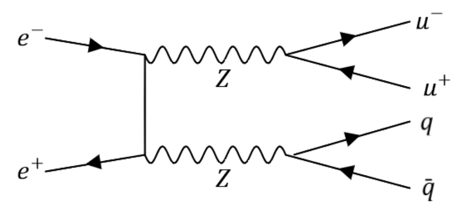

Figure 4: Feynman diagram - double Z resonance producing 4-fermion semi-leptonic output.

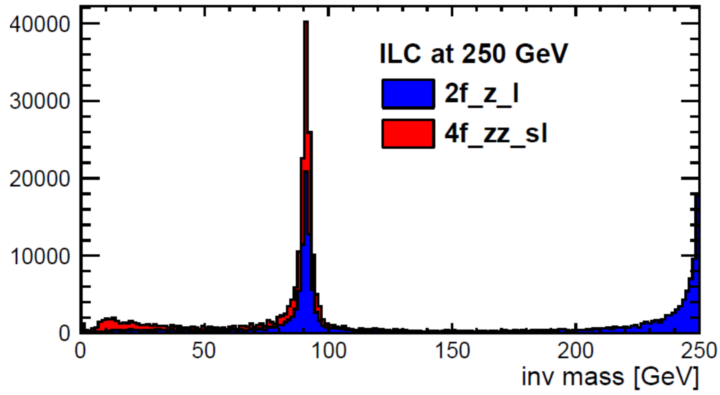

Figure 5: Isolated muon collection only - Dimuon spectrum for 2f-z-leptonic and 4f-zz-semi-leptonic, stacked plot.

This procedure led to the following plots in Figures 6 and 7 which plot the size of the PFO collection, (all reconstructed particle objects), for these two processes. Simply placing a cut where indicated would exclude a large number of events with hadronic output. There were an average of 14 PFOs per event for the 2-fermion, and 57 PFOs per event for the 4-fermion output.

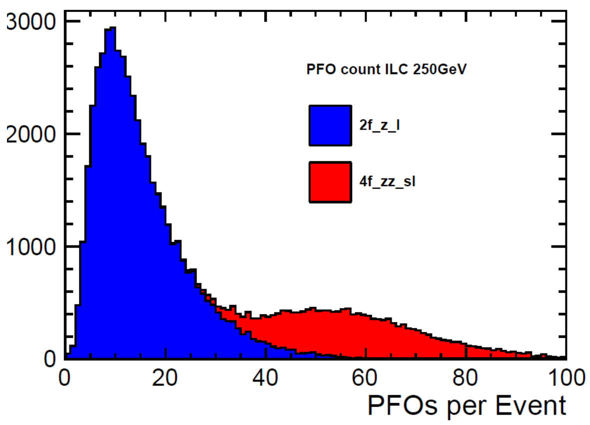

Figure 6: Size of PFO collection comoparison between 2-fermion leptonic and 4-fermion semi-leptonic events. (Stacked)

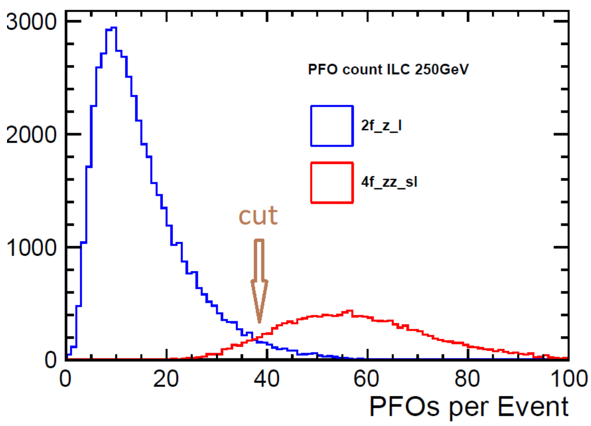

Figure 7: Size of PFO collection comoparison between 2-fermion leptonic and 4-fermion semi-leptonic events. (*nostack* applied).

One more potential background is shown in Figure 9: 2-fermion hadronic decays of the Z boson. This can demonstrate the potential for using the b-tagging parameter in LCIO to improve the signal to background ratio in certain narrow-peak cases; in particular, when pursuing the J/Ψ against this QCD background, after the generator level (Figure 9) J/Ψ have been excluded (The J/Ψ mass is ≈3GeV which has been cut at the generator level in this case). This approach could work because b-quarks, since they are lighter than the top quark, decay into either charm or up quarks. Both are Cabibbo suppressed, but b → up is doubly suppressed, meaning in reality the decay is to the charm. So potentially, using the b-tagging parameter in LCIO to identify secondary J/Ψ particles from b-jets, could improve the signal to background ratio of these secondary J/Ψ. This then relates directly to our search for the narrow Z' di-muon peak in our muon spectrum.

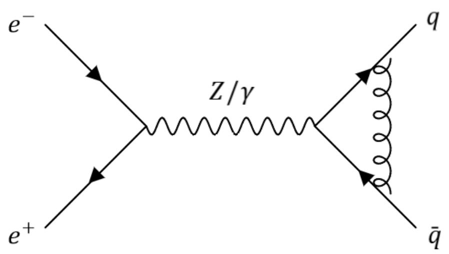

Figure 8: Feynman diagram - 2-fermion hadronic background.

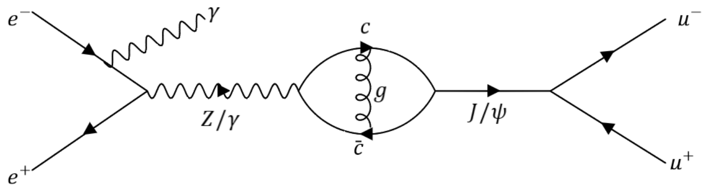

Figure 9: Feynman diagram - 2-fermion hadronic decay mode containing a J/Ψ, decaying in turn to a muon pair (BR≈ 6%)[5] after an ISR photon has reduced the e+e- system energy.

This works by cutting out any events in the refined2jets collection, where the b-value of both jets sum to less than 1. The b-value is the likelihood that a given jet came from a b-quark, so forcing this parameter is equivalent to requiring on average a 50% chance that each jet is a b-jet when taken together. Figure 10 shows the J/Ψ peak, including all paired PFOs reconstructed as muons, against the 4-fermion hadronic background with no b tagging applied to the jet collection. This is contrasted with the much more prominent peak in Figure 11, demonstrating the efficacy of this cut.

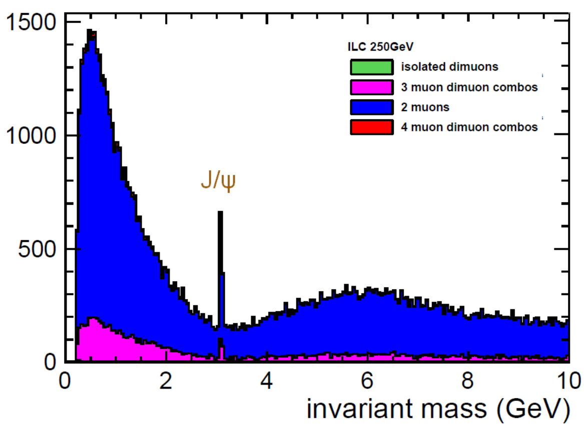

Figure 10: 4-fermion hadronic decay. All PFOs reconstructed as muons are included, paired up in all combinations of oppositely charged muon pairs.

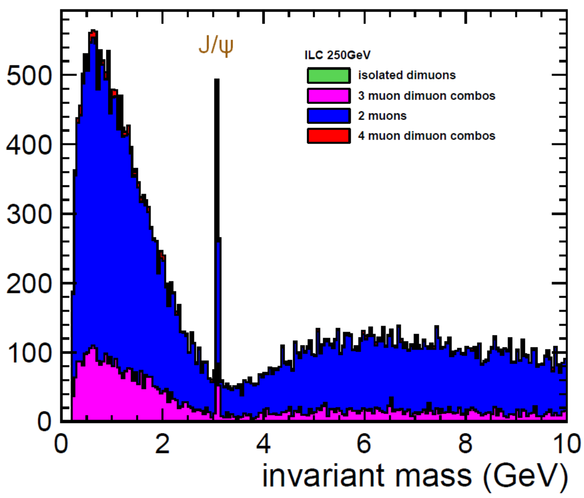

Figure 11: 4-fermion hadronic decay. All PFOs reconstructed as muons are included, paired up in all combinations of oppositely charged muon pairs, with B-Tagging applied.

2.2 Signal exclusion and detection

Now, I shift focus toward the final goal of being able to detect the generated signals at a range of dark photon masses, on top of the 2-fermion leptonic background, which is the dominating background. The question is what are the tolerances of ILC, that is, how much would the signal need to be scaled up or down at each point in the mass spectrum, to be excluded or detected at that point? To do this needed to ensure I had accurately weighted each event, based on the beam polarization. For this we use the cross section of an event, which we know from theory, and can be pulled from the DST files, and the integrated luminosity, which multiplied together give the number of events N expected for a process.

If we simulate 10 or 100 times the number of events expected in the 'real' data, to improve our statistics, we must therefore weight each event accordingly with 1/10 or 1/100. This gives the correct number of events in each bin, with weight:

$$\mathrm{w} = \frac{(\sigma \times \mathrm{L})}{\mathrm{N}}$$

Furthermore, the effective polarization of the beams needs to be accounted for. The convention is right helicity has value 1 and left has value -1. For example, given an electron beam right polarized (+1) only means that electrons are 80% polarized right, or they a value of 0.8. This means that 90% of the electrons will be right polarized, and 10% left polarized, which means they will have a different cross section to the one applied for the process. This comes down to how difficult it is to polarize the leptons successfully in a beam, and must be accounted for. The mathematics corresponding to the electrons in the example of a beam polarized to eRpL:

$$0.9 \times 1 + 0.1 \times (-1) = 0.8 \implies 90\% \text{ electrons have desired polarization.}$$

For the positrons:

$$0.65 \times (-1) + 0.35 \times 1 = -0.3 \implies 65\% \text{ positrons have desired polarization.}$$

Positrons are therefore more difficult to polarize. Spin conservation disallows LL and RR states; the initial state has spin=0, but the intermediate state of either a γ, a Z or a Z', is a spin-1 boson. We end up scaling the luminosities of these, and multiplying them with the appropriate cross sections to get the number of events expected:

$$\mathrm{L_{LR}} = L \times 0.9 \times 0.65,\ \mathrm{L_{RL}} = L \times 0.1 \times 0.35$$

$$\implies \text{Num of events } \mathrm{N} = \sigma_{\mathrm{LR}} \times \mathrm{L_{LR}} + \sigma_{\mathrm{RL}} \times \mathrm{L_{RL}}$$

Next, we seek the smallest signal which cannot be explained by a fluctuation in the background. Monte Carlo simulation will mean that in a given bin at a given energy, the number of events there will be described by a Poisson distribution. This is by definition the description of a probability distribution for independent events occurring with a known average rate. The expected number of events is then based on the theory of the standard model. Also, Poisson distributions tend toward Gaussian distributions when the stochastic variable is large, according to the central limit theorem[6]. With a Gaussian we know the probability to find an outcome at a certain number of standard deviations above expectation.

We define the minimum discoverable signal as: How big must a signal be, in number of events, for us to conclude that the observed number of events could not be a fluctuation of the expected background $< b >$ by itself ? We then define the minimum excludable signal as: How small can a signal's predicted number of events be $< s+b >$ such that the observed number of events represents too much of a downward fluctuation, and the signal should just be excluded, leaving only $< b >$ as the expected number of events?

To answer these, we conduct two separate hypothesis tests on the statistic which is the number of observed events, distributed as a Poisson (assumed Gaussian) distribution. Each test has a value x, against which the number of observed events is compared in order to decide what to conclude. x is determined by requiring that the probability of making the wrong decision is low. Table 2 highlights the differences between these tests.

Table 2 Comparison between hypothesis tests for discovery and exclusion

Discovery	**Exclusion**
H_0: no signal present ($s = 0$)	H_0: Signal present ($s > 0$)
H_1: signal found ($s > 0$)	H_1: Signal excluded ($s = 0$)
If N>x, reject H_0, discover signal	**If N<x, reject H_0, exclude signal**
Otherwise: accept H_0, no discovery	Otherwise: accept H_0, signal is present
Require if H_0 true: P(N>x)=1/1744278	Require if H_0 true: P(N<x)=0.05/2
Assume H_0 true: Let $R = \frac{N-b}{\sqrt{b}}$ P(R>x')=1/1744278 $\implies$ **x'=5**	Assume H_0: Let $R = \frac{N-(b+s)}{\sqrt{b+s}}$ P(R<x') = 0.025 $\implies$ **x'=-2**
Reject H_0 if N>$b + 5\sqrt{b}$	Reject H_0 if N<$s + b - 2\sqrt{(s+b)}$
If H_1 is true $\implies$ <N>= <s+b> $\mathbf{s>5\sqrt{b}}$	If H_1 is true $\implies$ <N>= <b> $\mathbf{s>2\sqrt{s+b}}$

The first test is characterised by a stringent requirement on the probability of rejecting H_0 if it is indeed true, with P(N>x)=1/1744278. This stringency is not necessary for an the second exclusion test, since claiming a discovery is a much more bold statement than the exclusion of a signal at some level. Also, note that the smallest expected signal for a discovery depends only on the number of background events, where as for exclusion, it depends on the signal and the background.

One example of a signal shown on the backgrounds with weights applied is shown in Figures 12 and 13. In this example, the window size of 50 MeV maximizes the number of standard deviations between H_0 and H_1, corresponding to the point to which one can most reduce the signal and still claim a discovery, for example. This gives minimum values for expected number of signal events for discovery and exclusion as:

$$s > 111 \text{ for DISCOVERY and } s > 46 \text{ for EXCLUSION.}$$

Figures 14 and 15 show the corresponding simulated plots of a 150 GeV Z' mass signal only output, and the signal plus background for this 50MeV window size example. Here there are 43024 signal muons 20269 background muons, leading to the expected discovery and exclusion limits:

$$s > 712 \text{ for DISCOVERY and } s > 285 \text{ for EXCLUSION.}$$

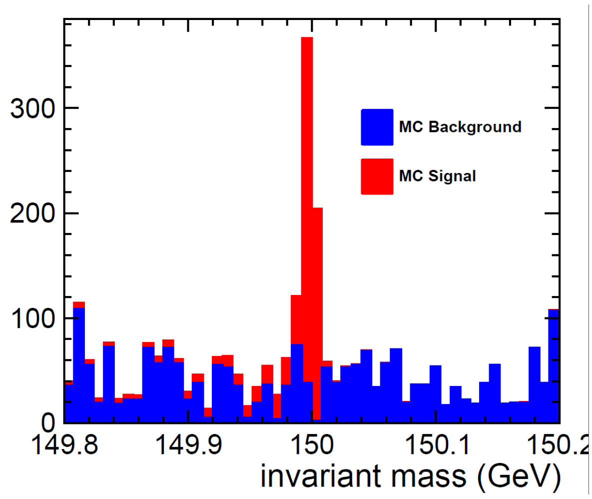

Figure 12: Z'=150GeV with a window size of 200MeV either side. 787 signal events and 2084 background events.

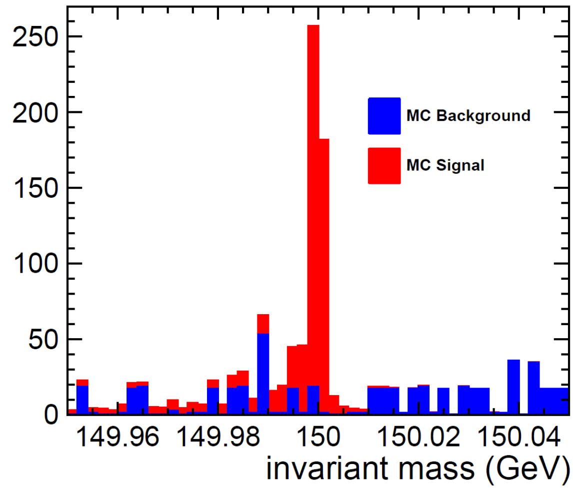

Figure 13: Z'=150GeV with a window size of 50MeV either side. 669 signal events and 498 background events.

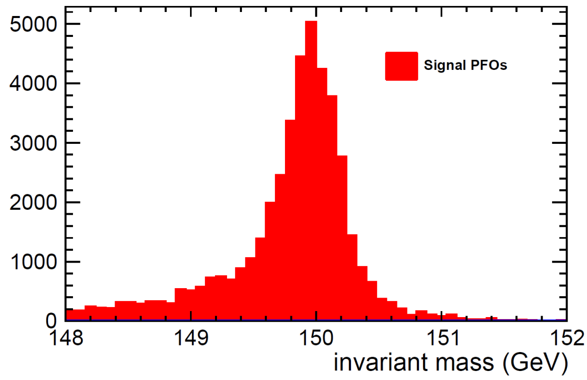

Figure 14: 150GeV SGV Signal only with 50 bins.

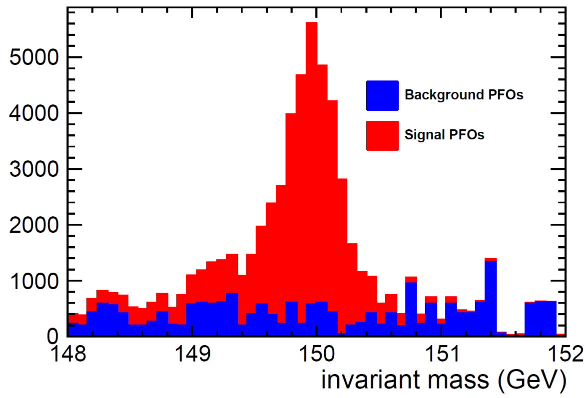

Figure 15: 150GeV Signal plus background with 50 bins.

To more accurately test the method of optimizing the window size with the best ability to determine the smallest signal, Table 3 shows a deeper preliminary analysis of the 150GeV Z' at the generator level only, resulting in the identification of an 18MeV window being the optimal window size. It would be a next step to repeat this for the signals that have been put through SGV detector simulation.

Table 3 Optimal window width at generator truth level for Z'=150GeV: 18MeV.

Width	Signal	BKG	s/sqrt(s+b)	Width	Signal	BKG	s/sqrt(s+b)
0.2	725.976	1025.15	17.3485	0.02	546.058	102.515	21.4417
0.18	717.913	922.639	17.7246	0.018	539.234	92.2639	21.4581
0.16	706.745	820.123	18.0868	0.016	529.468	82.0123	21.4116
0.14	695.729	717.608	18.5062	0.014	519.541	71.7608	21.3656
0.12	683.934	615.092	18.976	0.012	508.682	61.5092	21.3028
0.1	669.363	512.577	19.4699	0.01	494.572	51.2577	21.169
0.08	650.899	410.062	19.9831	0.008	475.664	41.0062	20.9264
0.06	628.26	307.546	20.5374	0.006	453.317	30.7546	20.6038

3 Concluding remarks and next steps

Having come to the end of our time alotment, the immediate next step would be to investigate the optimum window size for a signal post fast detector simulation. As well as that, the next step would be to plot all other Z' energies with a complete set of 2-fermion leptonic DST files, and to calculate the tolerances using the newly optimized windows size. Finally, adding in the other less dominant backgrounds would be very interesting, to see how the tolerances would change exactly. By adding the aforementioned 4-fermion semi-leptonic and 2-fermion hadronic backgrounds, I would expect the limits to require slightly more signal events for a discovery, and for the minimum expected value of a signal event exclusion also to increase. It would be informative to quantify exactly how much.

However, overall it has been very informative to see that over a range of Z' masses, a generated SGV signal should indeed be visible over the most dominant background of the 2-fermion leptonic decay mode. As well as that, I feel I have gained a huge amount from writing the code, and interacting with the ROOT framework to produce these plots and results.

4 Acknowledgements

Support, guidance and instruction on this project was provided by my supervisors Jenny List and Mikael Berggren, I am thankful for their dedicated time. I will also thank Jakob Beyer for his help.

References

[1] Ties Behnke et al. *The International Linear Collider Technical Design Report - Volume 1: Executive Summary*. 2013. arXiv: 1306.6327 [physics.acc-ph].

[2] *CERN LHC Description*. https://home.cern/resources/faqs/facts-and-figures-about-lhc. Accessed: 2021-08-25.

[3] Frank Gaede et al. “LCIO: A Persistency framework for linear collider simulation studies”. In: *eConf* C0303241 (2003), TUKT001. arXiv: physics/0306114.

[4] J. Reuter W. Kilian T. Ohl. *WHIZARD: Simulating Multi-Particle Processes at LHC and ILC*. Eur.Phys.J.C71 arXiv: 0708.4233 [hep-ph]. 2011.

[5] K. Nakamura. “Review of Particle Physics”. In: 37.7A (2010). An optional note.

[6] Hans Fischer. *A history of the central limit theorem: from classical to modern probability theory*. Springer Science & Business Media, 2010.

5 Appendix

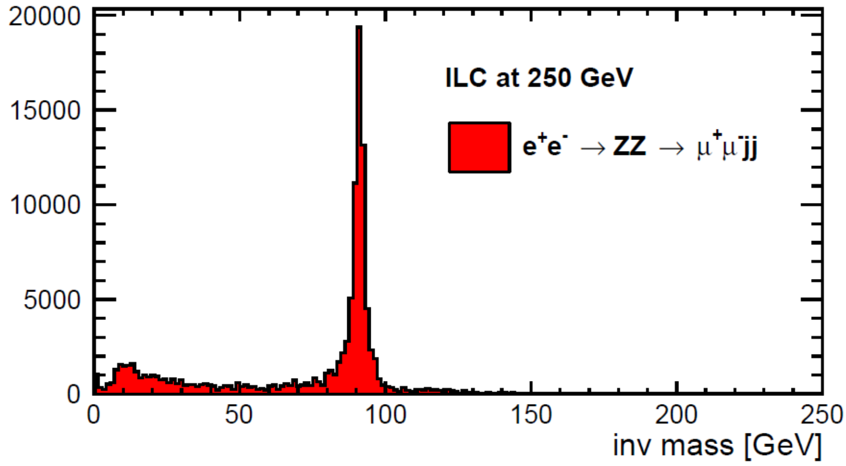

Figure 16: Isolated muon collection plotted for semi-leptonic, 4-fermion output. Only the Z-peak is visible in the isolated muon collection; the jets contain the remaining energy.(Average of 57 PFOs per event)

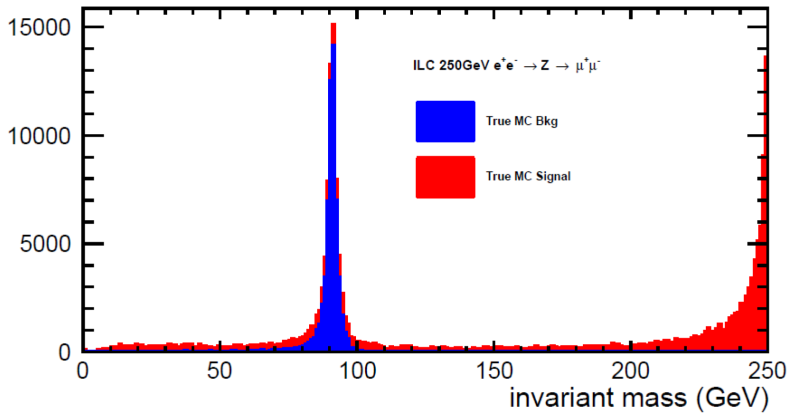

Figure 17: 2-fermion semi-leptonic signal to noise ratio; the corresponding MC particle is truly a muon. (Stacked).

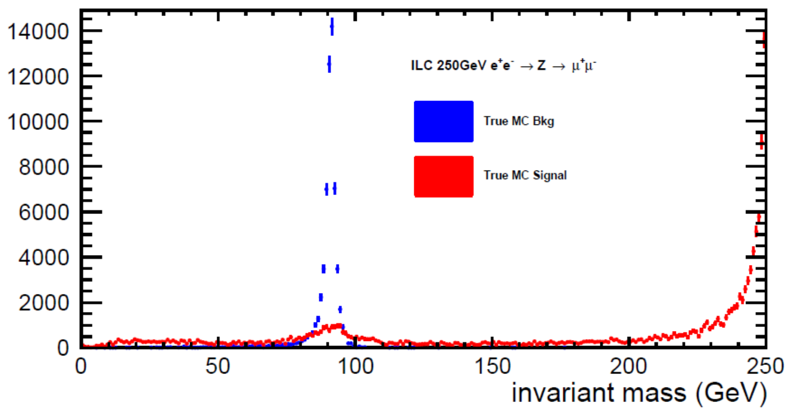

Figure 18: 2 fermion semi-leptonic signal to noise ratio; the corresponding MC particle is truly a muon. (*nostack* applied).

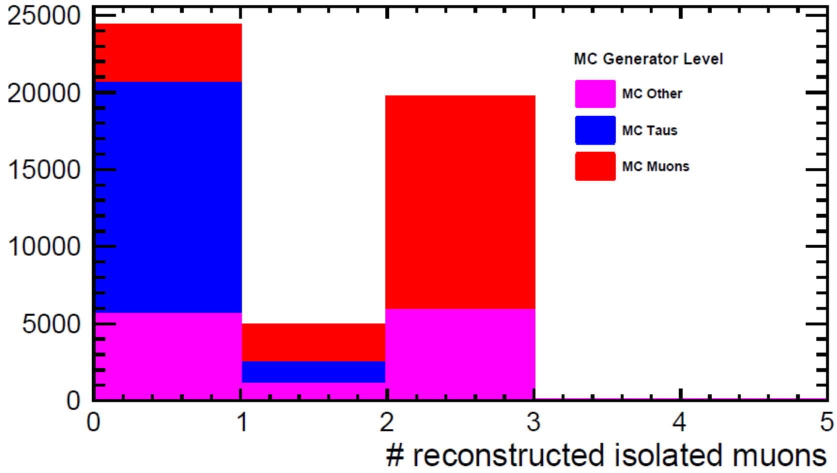

Figure 19: Size of isolated muon collection comparison between *true* (MC) Taus and *true* (MC) Muons, demonstrating the potential for another cutting parameter: keeping only events with 2 muons in the isolated muon collection would improve the accuracy of the reconstruction.

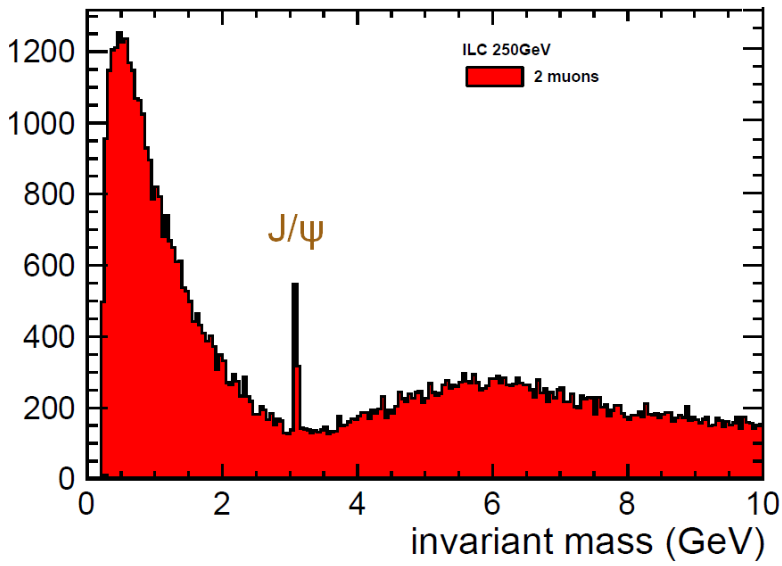

Figure 20: 4-fermion hadronic decay. Reconstructed 2 jet collection; di muons only. For reference comparison against Figures 10 and 11